Electronic Supplementary Information

Oxygen-deficient photostable Cu_2O for enhanced visible light photocatalytic activity

Mandeep Singh[a,†], Deshetti Jampaiah[a,†,*], Ahmad E. Kandjani[b], Ylias M. Sabri[b], Enrico Della Gaspera[c], Philipp Reineck[d], Martyna Judd[e], Julien Langley[e], Nicholas Cox[e], Joel van Embden[c], Edwin L. H. Mayes[f], Brant C. Gibson[d], Suresh K. Bhargava[b], Rajesh Ramanathan[a], Vipul Bansal[a,*]

[a]Ian Potter NanoBioSensing Facility, NanoBiotechnology Research Laboratory, School of Science, RMIT University, Melbourne VIC 3000, Australia

[b]Center for Advanced Materials and Industrial Chemistry, School of Science, RMIT University, Melbourne VIC 3000, Australia

[c]School of Science, RMIT University, Melbourne VIC 3000, Australia

[d]ARC Centre of Excellence for Nanoscale BioPhotonics, School of Science, RMIT University, Melbourne VIC 3000, Australia

[e]Research School of Chemistry, Australian National University, Canberra VIC ACT 30002601, Australia

[f]RMIT Microscopy and Microanalysis Facility, School of Science, RMIT University, Melbourne VIC 3000, Australia

[†]*Equal contributing authors*

[*]*E-mail: vipul.bansal@rmit.edu.au; jampaiah.deshetti@rmit.edu.au*

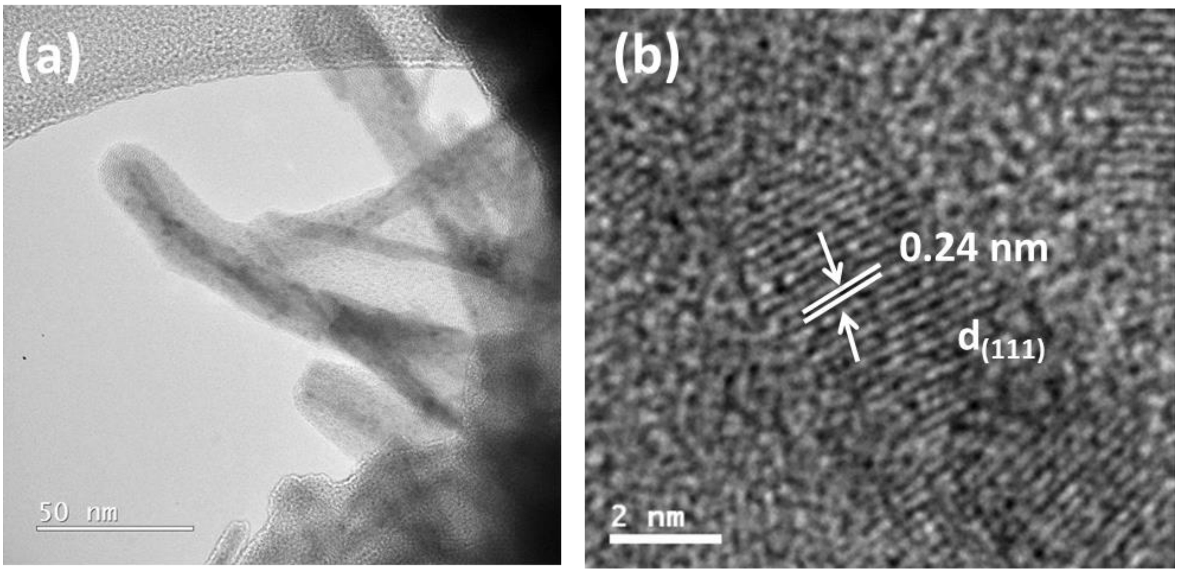

Fig. S1 HR-TEM images of Cu_2O nanotubes formed after 10 sec of reaction at room temperature.

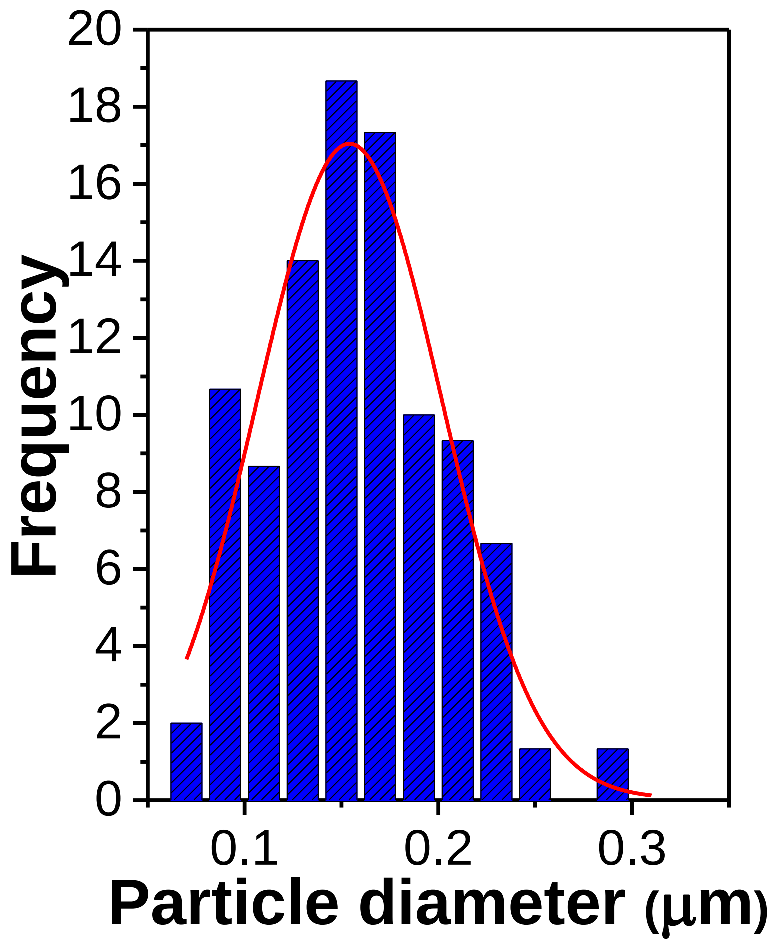

Fig. S2 Particle size distribution of as-synthesised Cu_2O nanoparticles, as determined by SEM.

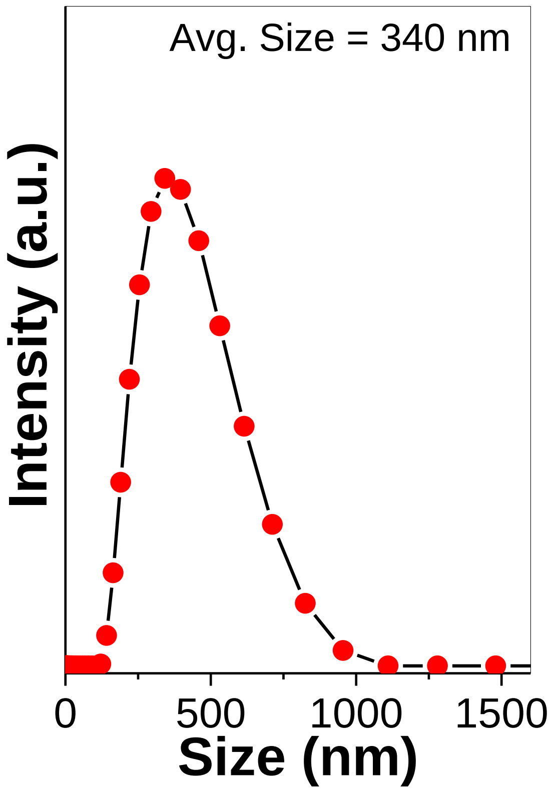

Fig. S3 Hydrodynamic diameter of as-synthesised Cu_2O nanoparticles in water, as determined by DLS.

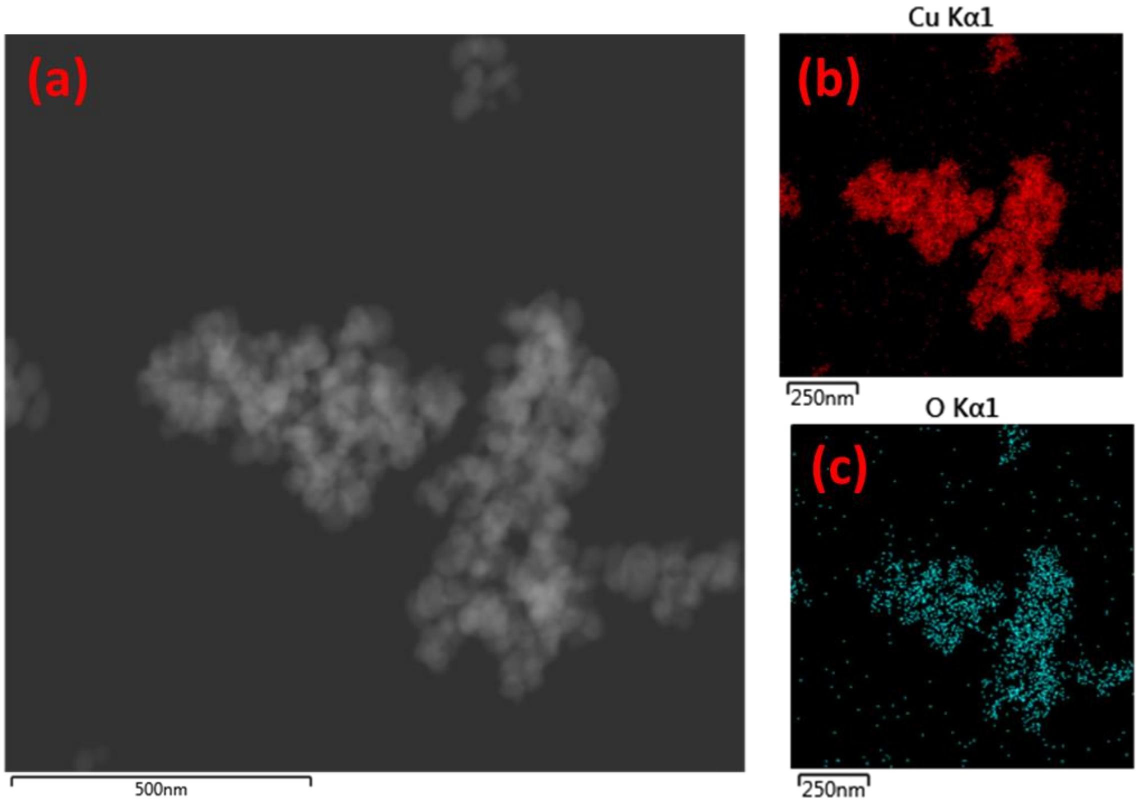

Fig. S4 EDX mapping of as-synthesised Cu_2O nanoparticles obtained on a nickel TEM grid.

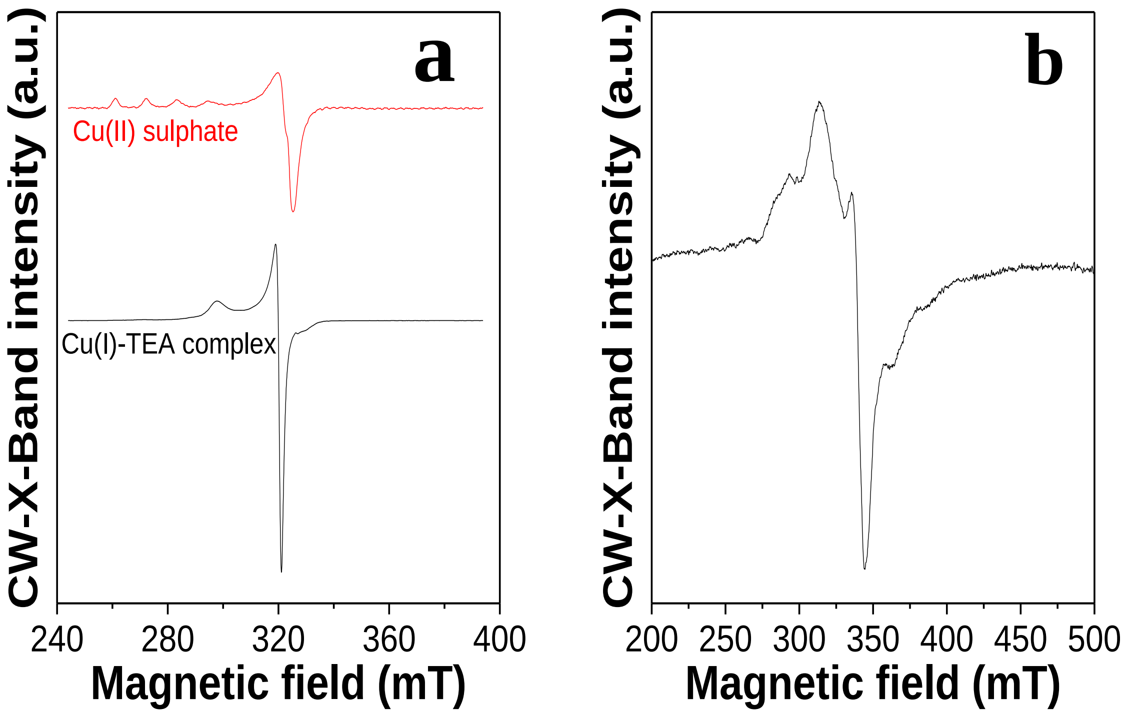

Fig. S5 (a) Low-temperature (20 K) CW-X-Band EPR spectra of the Cu(I)-TEA complex and CuSO4 standard. The spectra have been scaled for clarity. Instrument settings: microwave power – 63 μW; and field modulation amplitude – 2.0 mT; (b) Room-temperature CW-X-Band powder EPR spectra of oxygen-deficient Cu_2O nanoparticles. The baseline (EPR spectrum of the empty resonator) is subtracted from the obtained trace. Instrument settings: microwave power – 6.3 mW; and field modulation amplitude – 1.0 mT.

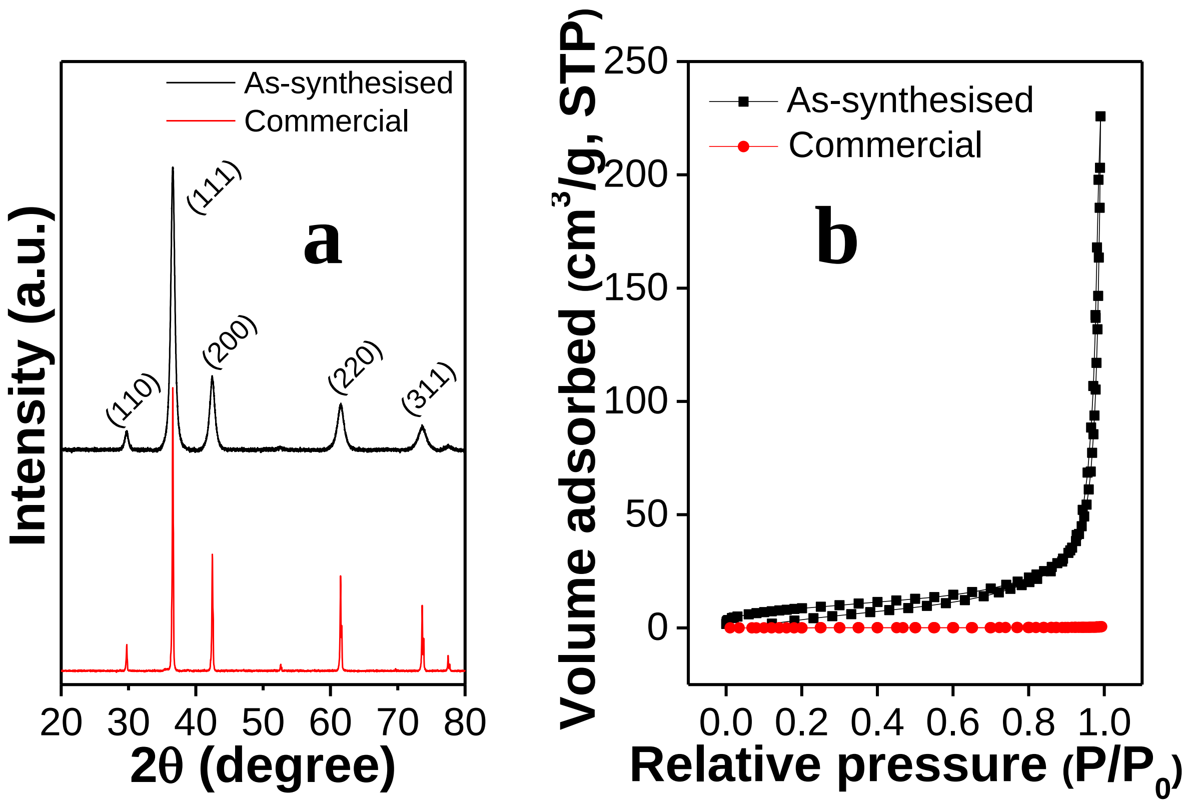

Fig. S6 (a) Powder XRD, and (b) N_2 sorption isotherms of as-synthesised Cu_2O nanoparticles and commercial Cu_2O.

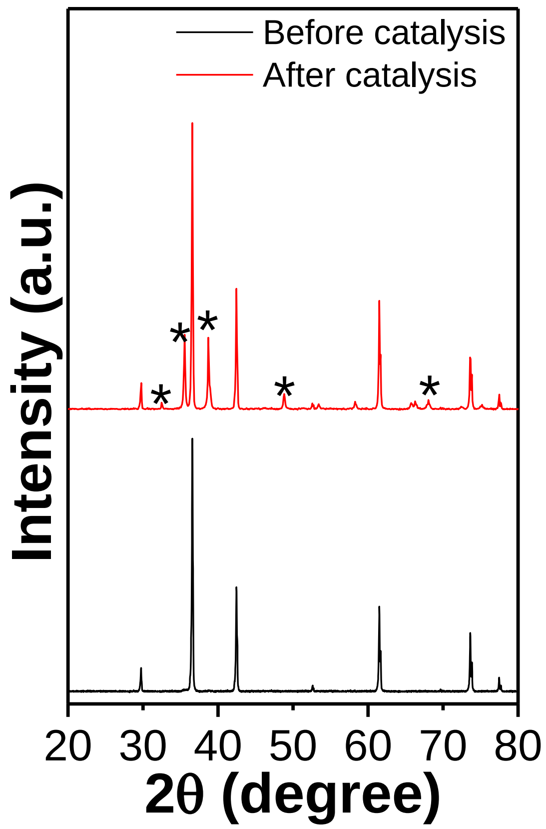

Fig. S7 XRD patterns of commercial Cu_2O nanoparticles before and after visible light-induced photooxidative degradation of methyl orange. The appearance of CuO signatures (marked with *) after photocatalysis reaction due to oxidation of commercial Cu_2O are noted.

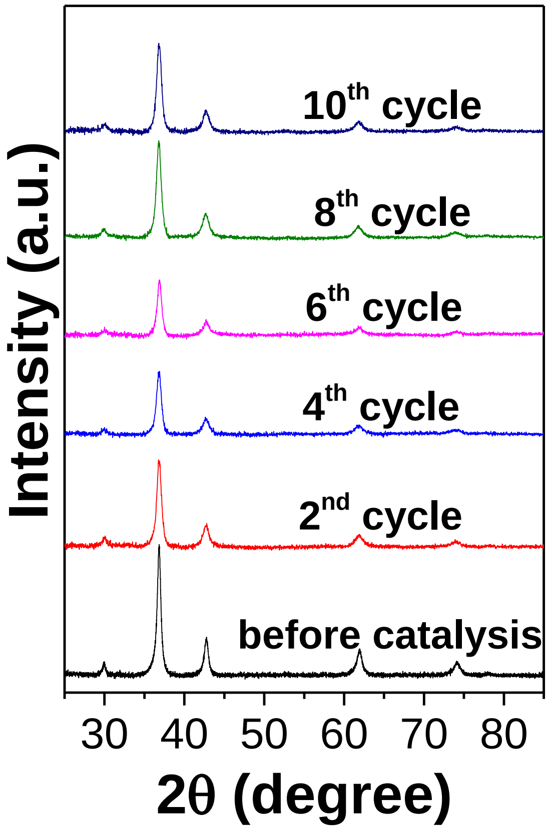

Fig. S8 XRD patterns of as-synthesised oxygen-deficient Cu_2O nanoparticles after repeated cycles of visible light-induced photo-oxidative degradation of methyl orange.

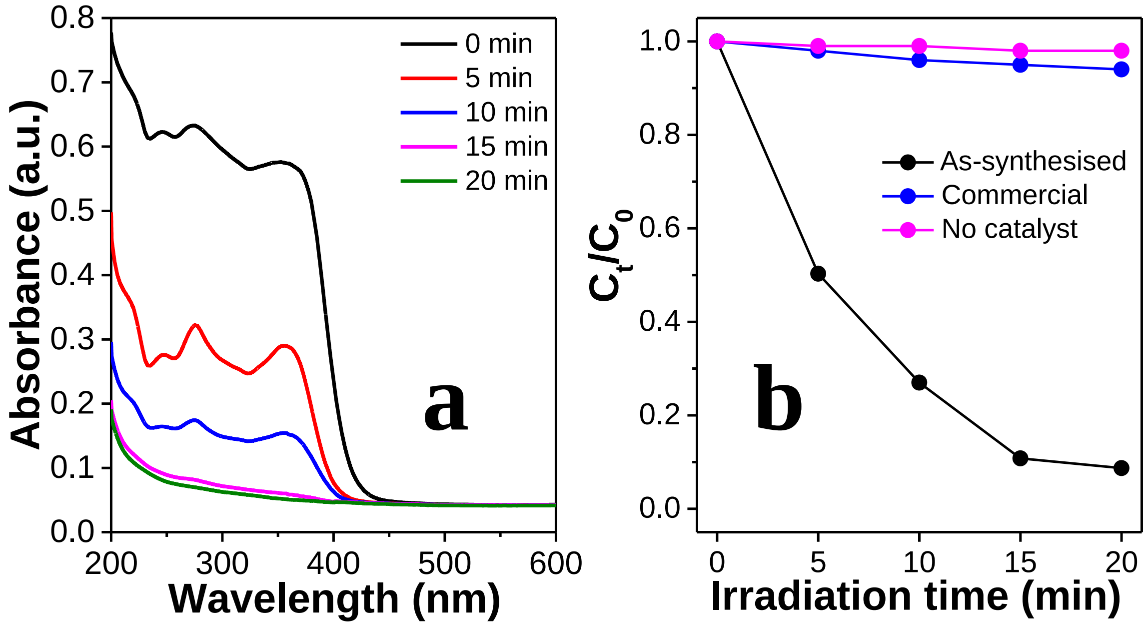

Fig. S9 (a) Photo-oxidation of tetracycline using oxygen-deficient Cu_2O, as evident from the UV-Vis absorption spectra of tetracycline after visible light photo-irradiation over 20 minutes; (b) plots of Ct/C0 vs. irradiation time depicting the photodegradation of tetracycline in the presence of different catalysts.

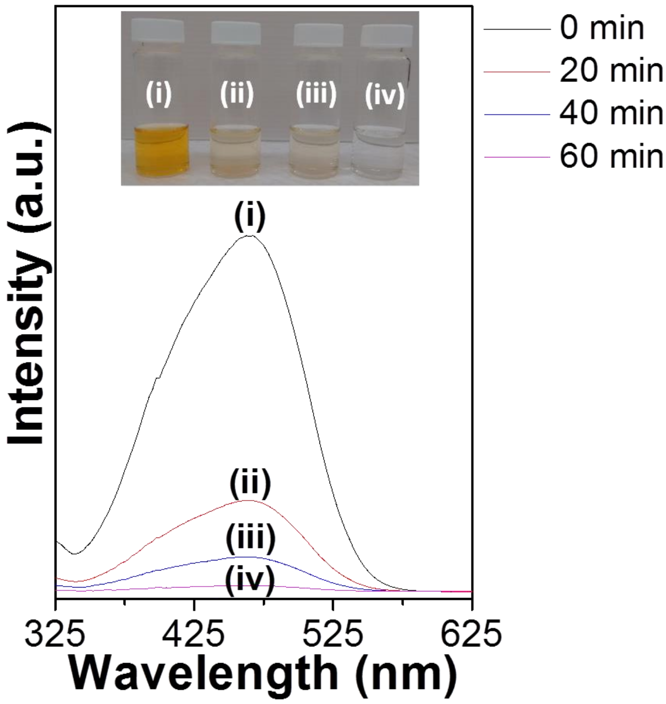

Fig. S10 Absorption spectra of MO over 1 h of exposure to simulated solar light in the presence of oxygen-deficient Cu_2O nanoparticles. Insets show the colours of the corresponding solutions.

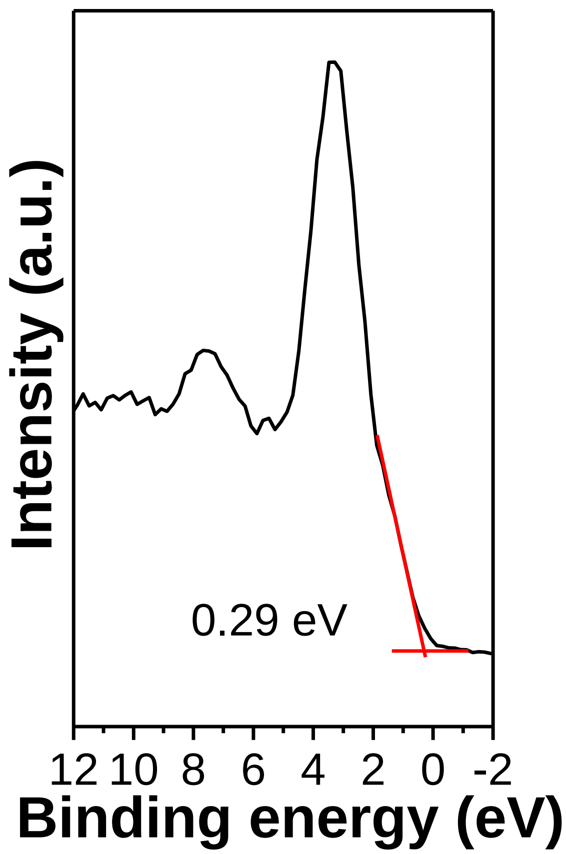

Fig. S11 Valence band XPS spectrum of oxygen-deficient Cu_2O nanoparticles.

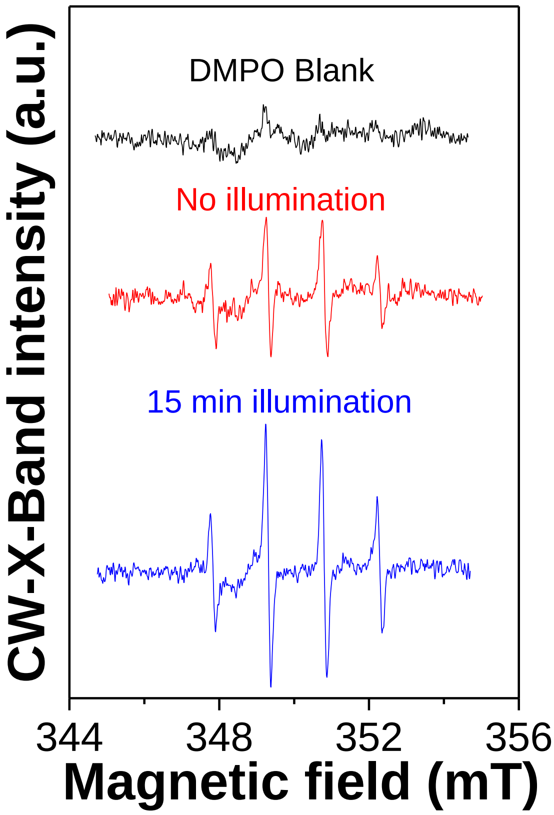

Fig. S12 Liquid solution CW-X-Band EPR Spectra of the DPMO-OH adduct generated by white light illumination of oxygen-deficient Cu_2O nanoparticles. Top trace: DMPO solution with no Cu_2O added; middle trace DMPO/Cu_2O reaction mixture before exposure to light; bottom trace DMPO /Cu_2O reaction mixture after 15 min illumination. Instrument settings: microwave power – 200 mW; and field modulation amplitude – 0.1 mT.

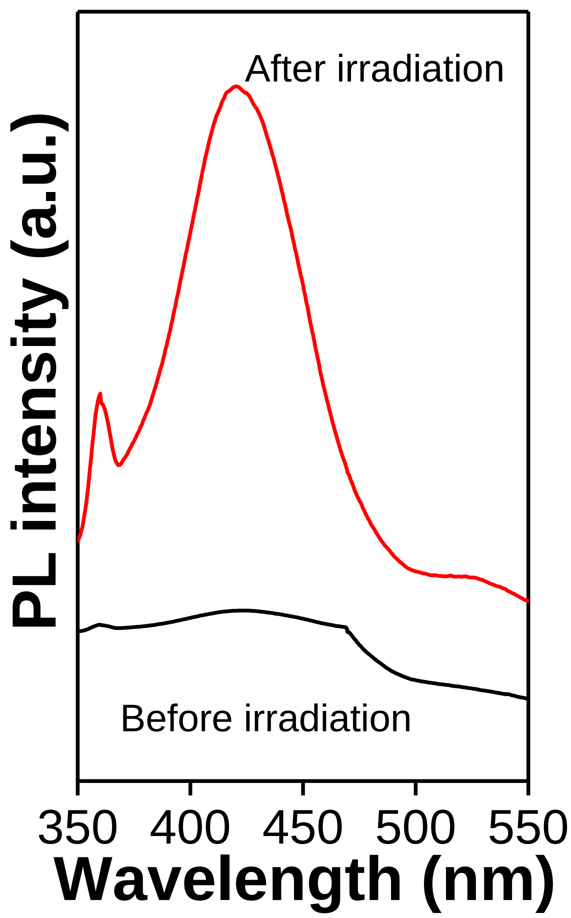

Fig. S13 Fluorescence spectra of 3 mM terephthalic acid (TA) obtained in the presence of oxygen-deficient Cu_2O nanoparticles at the λ_{ex} of 320 nm. Before photoexcitation, TA molecules remain non-fluorescent; however after 15 min of visible light photoexcitation, the $OH^{\bullet}$ radicals generated by the photo-excited Cu_2O nanoparticles readily react with TA to produce highly fluorescent 2-hydroxy terephthalic acid (λ_{max} ~425 nm).

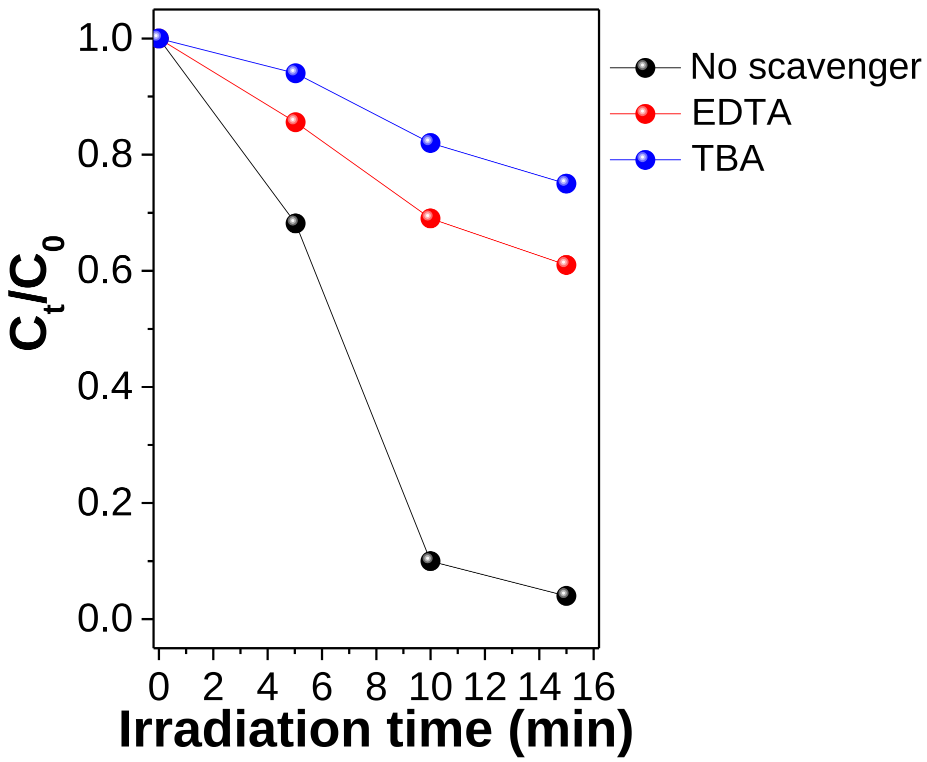

Fig. S14 Plots of C_t/C_0 versus irradiation time for oxygen-deficient Cu_2O nanoparticles-driven MO photodegradation in the presence of different scavengers. EDTA and TBA are able to supress the photo-oxidation efficiency to 38% and 25%, respectively, in comparison to the control reaction involving no scavenger.

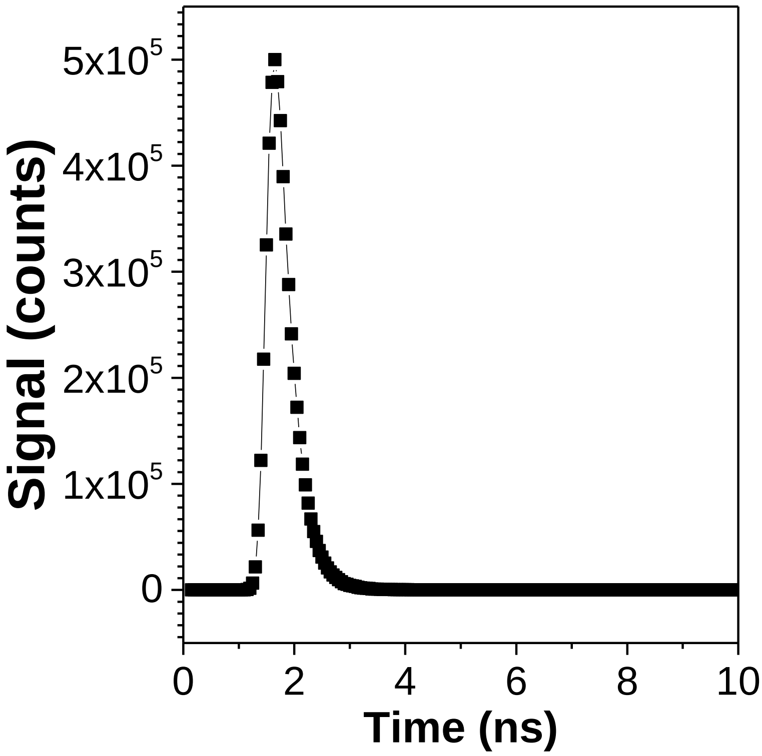

Fig. S15 Instrument response function (IRF) for the instrument used to acquire the time resolved PL spectrum of Cu_2O nanoparticles.

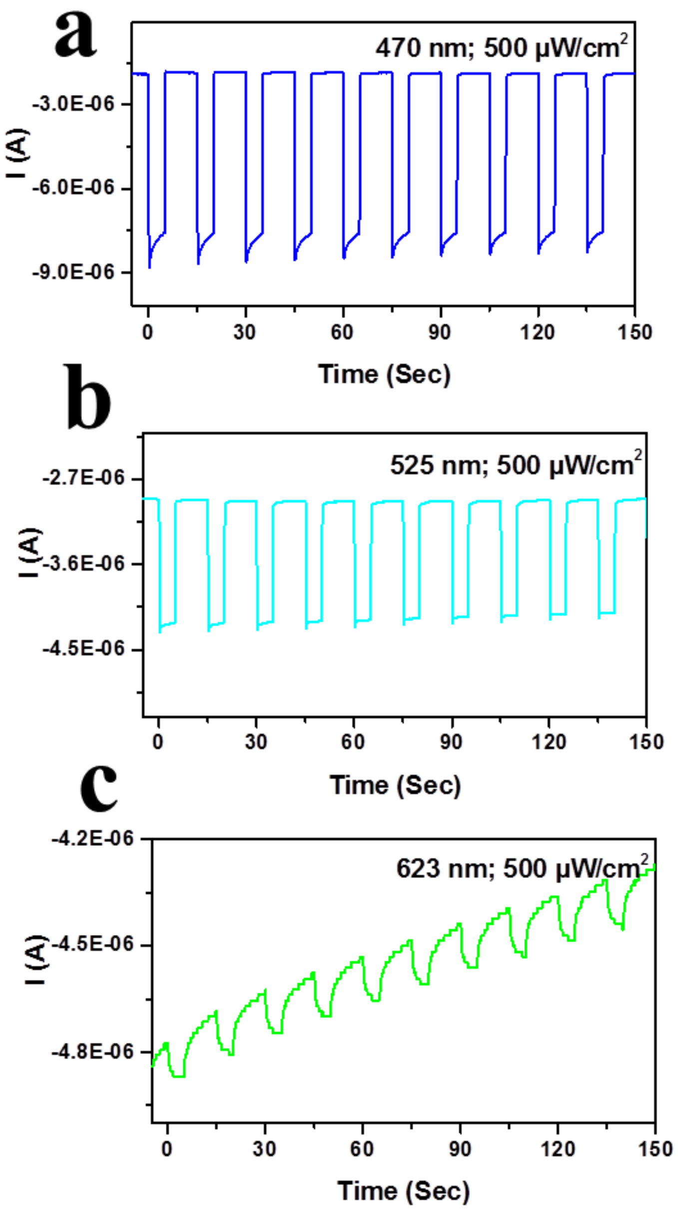

Fig. S16 The dynamic photocurrent response repeatability of the substrate over 10 exposure cycles of constant intensity of 500μW•cm^{-2} for wavelengths of **(a)** 470 nm, **(b)** 525 nm, and **(c)** 623 nm.